Journal of Membrane Science and Research 3 (2017) 187-198

Journal of Membrane Science & Research

journal homepage: www.msrjournal.com

Review Paper

Nanocomposite Membranes with Magnesium, Titanium, Iron and Silver Nanoparticles - A Review

Lakshmeesha Upadhyaya, Mona Semsarilar, André Deratani, Damien Quemener*

IEM (Institut Europeen des Membranes), UMR 5635 (CNRS-ENSCM-UM2) Université Montpellier, Place E. Bataillon, F- 34095, Montpellier, France

Article info

Received 2016-09-23
Revised 2016-12-15
Accepted 2017-01-19
Available online 2017-01-19

Keywords

Nanocomposite membranes
Inorganic nanoparticles
TiO_2 NPs
Fe_2O_3 and Fe_3O_4 NPs
Ag NPs

Highlights

- Nanocomposite filtration membranes
- Inorganic nanoparticles as filler in polymer films
- Applications of nanocomposite membranes

Graphical abstract

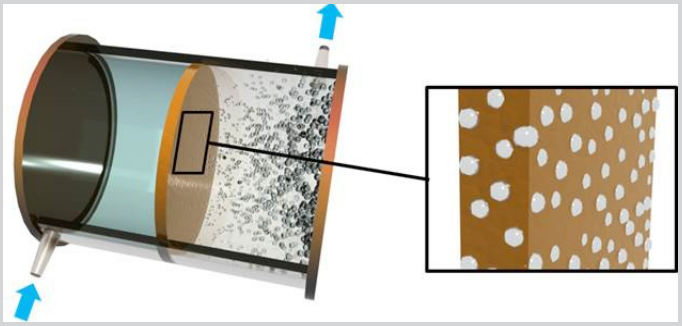

Abstract

Nanocomposite membrane comprising of both organic and inorganic material qualities have become a prime focus for the next generation membranes. Nanocomposite may consist of hard permeable or impermeable inorganic particles, such as zeolites, carbon molecular sieves and, silica and carbon nanotubes, metal oxide blended with continuous polymeric matrix presents an attractive approach for improving the separation properties of polymeric membranes. In this review, we have specifically focused the discussion on metal oxides like MgO, Fe_2O_3, Fe_3O_4, and TiO_2 along with silver NPs as filler in the formation of Nanocomposite membrane. The effects of these fillers on membrane characteristics, structure and performance using different applications have been discussed.

Contents

* Corresponding author at: Phone: +33 (0)4 67 14 91 22; fax: +33 4 67 14 91 19
E-mail address: damien.quemener@umontpellier.fr (D. Quemener)

DOI: 10.22079/jmsr.2017.23779

1. Introduction

In early 1960 to 70, rapid growth in membrane technology has been observed with the use of polymeric and inorganic membranes in which polymeric membranes were extensively utilized for both gas and liquid applications [1]. The biggest problem faced by polymeric membranes are their mechanical durability and chemical resistance needed for many industrial applications [2-4]. The alternative will be the use of inorganic membranes which has excellent separation efficiency along with the chemical and thermal stability. However, the cost related to their preparation as well as processability are the major challenges related to these membranes. So, the requirements of new membrane materials with improved characteristics made the development of nanocomposite membranes with combined properties of inorganic such as thermal stability, higher mechanical strength, along with the qualities of polymers like flexibility and processability [1,5,6].

In 1988, Kulprathipanja et al., [7] demonstrated the 1st prototype of nanocomposites based membranes made of cellulose acetate and silicate blend for CO_2/H_2 separation where silicate helped to reverse the selectivity of cellulose acetate membrane from H_2 to CO_2. These membranes have potential application in the field of separation of nitrogen from the air and CO_2 from natural gas [1,3,5,6,8-17], separation of liquid mixture like ethanol-water by pervaporation [18,19], reducing the fouling phenomena [20]. There are series of inorganic fillers available to blend with polymeric matrixes like molecular sieves (e.g. Zeolite, Metal Organic framework's, activated carbon, silica's, metal oxides, activated carbon, polyethylene glycol, ionic liquids) [1-6,8,10,11,16,20-25].

After the most promising literature by Zimmerman et al., [1] several reviews on nanocomposite membranes focusing on the current state of the art of hybrid membrane as an alternative to membrane materials for separation process, have been issued [2,3,5,14,29,30]. In this review, we have concentrated specifically on metal oxides like MgO, Fe_2O_3, Fe_3O_4, and TiO_2 along with silver NPs as filler in the formation of nanocomposite membranes. Silica was the great filler during initial stages that its addition was then replaced by metal oxides like MgO, TiO_2 which are the first metal nanoparticles used in nanocomposite membranes fabrication [2]. These nanoparticles of metal oxides have a higher surface area which increases uniform distribution of the particle over matrix along with non-selective void formation between the NPs surface and the matrix interface.

2. How to prepare?

The nanocomposite membranes could be symmetric or asymmetric as shown in Figure 1 [6]. The symmetric nanocomposite membranes preparation needs good dispersion of inorganic particles (INP) in the organic phase with optimal loading. In the case of asymmetric membranes, there will be a dense selective layer on a porous support which decreases the membrane resistance for transport of molecules [1]. The asymmetric membranes were prepared by synthesizing thin top layer with a careful deposition of INPs in it, whose size similar to the scale of the top layer as shown in Figure 1 which increases the capacity of particle loading thereby increasing its surface to volume ratio. The use of particular type of nanocomposite membranes depends on upon what kind of mass transfer one can expect for a particular operation [6].

The casting solution preparation is one of the important steps in the synthesis of nanocomposite membrane because of the presence of two different phases. The compatibility between the polymeric and inorganic phase, the universal solvent, their viscosity, loading and many more critical parameters will affect the final membranes prepared. The particle size used for the preparation of membrane is one more factor to be considered. When smaller particles are used, their higher surface/volume ratio enhances the mass transfer between the two phases. After addition of particles into casting solution, the even distribution of particles in the final membranes is needed to have optimal performance. When high particle loading is reached, an agglomeration is observed which increases the diffusion distance between the agglomerate [1,26-28]. The mixed matrix membranes are a hybrid membrane that may contain solid, liquid or both in polymeric phase. The presence of an additional phase will increase the selectivity as well as permeability along with processability of the polymeric membrane. Koro's et al. [29] has well explained the estimation of permeability for mixed matrix membrane through Maxwell model.

$$P_{MM} = (P_D + 2P_M - 2Q_D(P_M - P_D))/(P_D + 2P_M + 2Q_D(P_M - P_D)) \quad (1)$$

where P corresponds to permeability, Q_D is volume fraction, the subscript D and M corresponds to dispersed and continuous phase. This equation will allow us to match the physical and chemical properties of organic and inorganic phase to get the needed enhancement in the final membrane.

Figure 2 shows different possibilities of synthesis of nanocomposite membrane using INPs and polymer matrix. The synthesis procedure starts with preparation of a homogeneous mixture of polymer and inorganic particles. There are three possibilities of doing it. In one, INPs are dispersed in a solvent under stirring followed by addition of polymer. The second possibilities are to dissolve the polymer in a suitable solvent followed by addition of fillers, or final strategy will be inorganic particles and polymer solution in a suitable solvent prepared separately followed by mixing them. Figure 1 shows the detailed procedure in which the 1st and third methods used to make an even distribution of filler molecules because of no agglomeration since the solutions are very dilute [3].

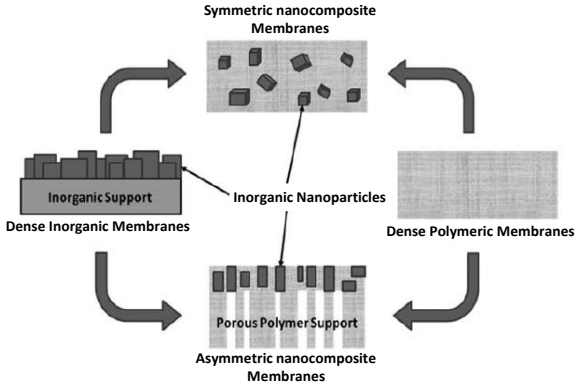

Fig. 1. Different types of nanocomposite membrane morphologies. (Adapted from [6]).

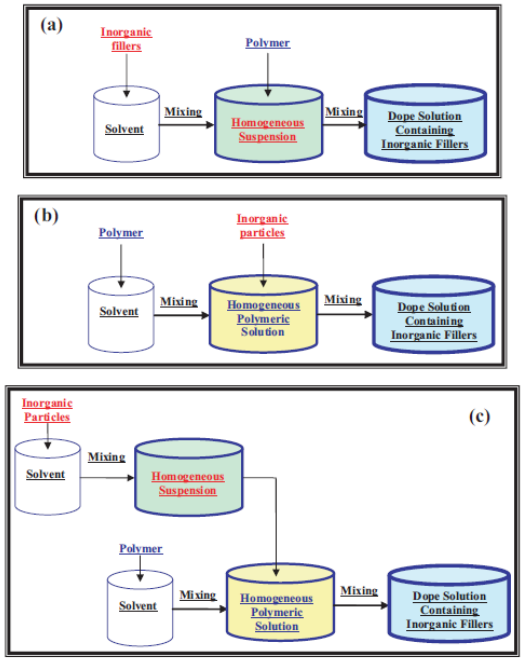

Fig. 2. Different strategies to prepare MMMs casting solution preparation (Reprinted from [3]).

3. MgO as filler

The affinity and interaction between MgO NPs and the gas molecule primarily CO_2 provide great potential for the use of MgO as filler. Hosseini et al. [31] used MgO as filler in the synthesis of nanocomposites for the first time with Matrimid® in 15 wt% concentration for dehydration of isopropanol by pervaporation. The nanosized crystallites of MgO surface interfered with the polymer packing inducing the chains rigidification. The Matrimid®/MgO nanocomposite membrane shown higher selectivity, but lower permeability compared to the original Matrimid® dense membrane. The greater selectivity was mainly due to the selective sorption and diffusion of water in the MgO particles, and properties change because of particle–polymer interface. The membranes were used for pervaporation of isopropanol containing 10 wt% water, the selectivity of the hybrid membrane is around 2,000, which is significantly increased as compared to the corresponding all polymeric membrane having a selectivity of 900.

In 2008, Matteucci et al. [32,33] used the MgO INPs in poly(butadiene) creating a polymer composite showing influence on CO_2, CH_4, N_2 and H_2 permeability by differential nanoparticle loading. The enhanced gas diffusivity was related to the high porosity of MgO particles embedded in the matrix. An increase in permeability was observed which is related to the microvoids at the polymer-particle interface as well the transport properties of highly porous MgO itself creating pore size greater than kinetic diameters of the gas molecule. The CO_2 permeability was increased from 52 barrer in the polymer membrane made of poly(butadiene) to 650 barrer in hybrid membrane containing 27 vol% of MgO. The highly porous MgO particle not only increased the transport properties of CO_2 but also shown the higher adsorption capacity towards CO_2 molecule.

Momeni et al. [11] used the nanocomposite membranes made of polysulfone blended with MgO INPs synthesized by phase inversion technique for gas separation application. The T_g of nanocomposite membranes increased with MgO loading because of low mobility of MgO and higher stiffness of the particles, the mobility of polymer chain decreased. The particle incorporation increased the permeability of gas molecule which shown the growth behavior as the particle loading increased which is shown in Figure 3A and 3B. The results of gas permeation revealed that the increase in permeability was correlated to INPs addition. At 30 wt% MgO loading, the CO_2 permeability was increased from 25.75×10^{-16} to 47.12×10^{-16} mol.m/(m^2.s.Pa) and the CO_2/CH_4 selectivity decreased from 30.84 to 25.65 in comparison with pure polysulfone membrane. For H_2, the permeability was enhanced from 44.05×10^{-16} to 67.3×10^{-16} mol.m/ (m^2.s.Pa), whereas the H_2/N_2 selectivity decreased from 47.11 to 33.58. The detailed analysis is provided in Figure 3.

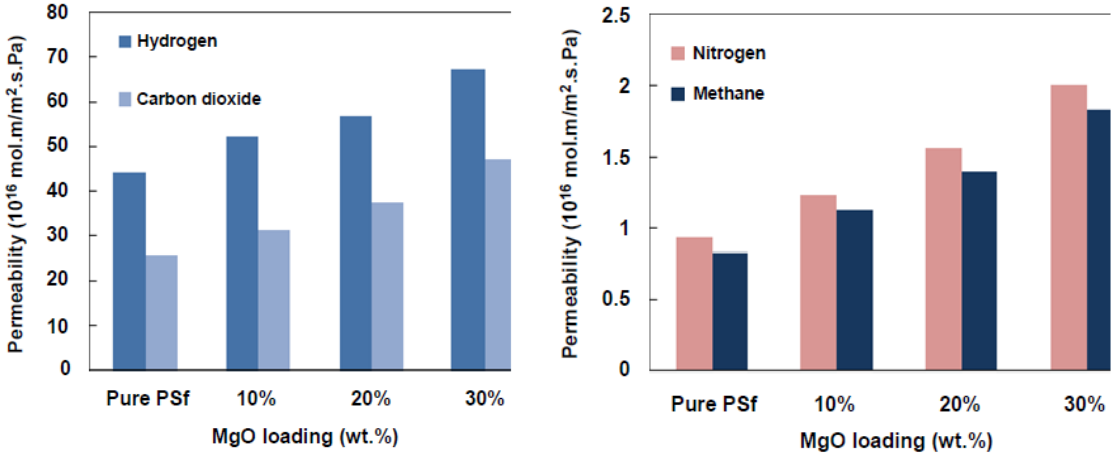

Fig. 3. The comparison of gas permeability for polysulfone-MgO composite membrane (Reprinted from [11]).

Othman et al. [34] synthesized the membrane by mixing epoxidized natural rubber (ENR) and polyvinyl chloride (PVC) with MgO as filler. With pure polymer membranes, no pores were observed, but the addition of MgO created pores in the mixed matrix membranes. ENR/PVC with 2% MgO membrane had pores with a diameter ranging from 1.3-1.6 μm. The pore diameter of ENR/PVC with 5% MgO membrane increased from 1.6-1.8 μm, while the pore diameter of ENR/PVC with 8% MgO membrane increased from 1.4-2.9 μm. The presence of pore inside the membranes was due to the substitution of dense structure brought by polymer chains by highly porous MgO. As the amount of MgO was increased, the more compact structure was substituted. The permeation capacity of ENR/PVC was increased by the addition of MgO. The selectivity of the membrane is detailed in Table 1. The selectivity of CO_2 over N_2 was increased mainly because of acidity of CO_2 resulting in higher affinity for physisorption towards MgO which increased the permeability and selectivity.

Table 1
Selectivity of CO_2/N_2 for all membranes

Pressure (bar)	ENR/PVC	ENR/PVC with 2% MgO	ENR/PVC with 5% MgO	ENR/PVC with 8% MgO
2	3.0	1.8	1.3	1.2
4	2.0	2.0	1.4	1.4
6	1.7	2.1	1.5	1.4

4. TiO_2 as filler

Significant research has been carried out on TiO_2 NPs over the last five decades and is more attractive because of its low cost, photostability in solution, nontoxicity, redox selectivity and strong oxidizing power as well photocatalytic and antimicrobial properties. The use of TiO_2 as filler in the synthesis of mixed matrix membrane become an attractive and profitable technique. The INPs as filler mainly used for gas separation as well to reduce fouling.

Matteucci et al. [35] used the TiO_2 particle surface chemistry on the gas transport properties of the MMMs by taking both glassy and rubbery system as an example. At lower doping concentration the characterization revealed that the particles dispersed individually whereas in high doping concentration they were seen as small micron-sized aggregate. When the application of these composite membrane was tested for gas separation, the diffusivity and selectivity of CO_2 and nonpolar gas were increased by increasing the INPs load. The reason for the increase in permeability was mainly due to the void formation at nanoparticles– polymer matrix interface, agglomeration of particles and weak interaction between polymer–nanoparticles at the interface during high loading conditions. Overall, there was a decrease in selectivity of nanocomposite made of Matrimid compared to pure Matrimid membranes. In the case of CO_2, the permeability enhancement of Matrimid containing 20 vol% TiO_2 was 2.45 times higher than neat Matrimid, while CO_2/CH_4 selectivity decreased by 33%, revealing that the use of TiO_2 nanoparticles improved membrane performance in CO_2/CH_4 separation.

Similar results have been seen in the work of Moghadam et al. [12] where Matrimid 5218 was doped with INPs. About 15% loading, ensured

individualization of the INPs whereas, above 20%, detrimental aggregation was reported. As the INPs loading was increased because of weak organic and inorganic particles interaction at lower loading, the particle distribution was uniform whereas at higher loading the particles started voids and micron sized aggregates. The size of the aggregate was increased from 250 nm to 0.5 µm when the loading was increased from 15% to 20%. Even the elongation and tensile strength of the nanocomposite membranes were decreased. The 15 wt% of INPs containing membrane shown about 2.76, 3.3 and 1.86 times increase in permeability compared to the pure Matrimid for N_2, CH_4 and CO_2 respectively. This is due to the change in free volume and void spaces. The nanoparticle loading disrupts the chain packing and changes the structural regularity at nanoparticle-polymer interface leading to the free volume variation.

Soroko et al. [19] developed nanocomposite membranes by doping TiO_2 in polyimide by using *N*, *N*-dimethylformamide/ 1,4-dioxane solvent mixture and observed the changes in hydrophilicity of the membrane because of highly porous TIO_2. The macro voids in pure PI membranes were eliminated after addition of TiO_2 particles (loading above 3 wt%). The INPs in the doping solution increased its viscosity significantly because of their higher specific area and surface energy. This increase in viscosity acted as void suppressing factor because of lowering in the exchange rate of solvent-non-solvent and delayed liquid-liquid demixing. The addition also enhanced the hydrophilicity of the membranes and compaction resistance, whereas rejection and flux remained same.

One more usage of doping TiO_2 was to decrease the fouling effect which is initially studied by Kwak et al. [36]. They synthesized reverse osmosis membrane consisting of aromatic polyamide thin films with titanium dioxide INPs by a self-assembly process. The sol-gel procedure was used to synthesize the nanoparticles with a diameter of 2-10 nm with anatase crystallographic form. The membrane showed the improved water flux behavior whose antibacterial fouling potential was tested by the survival ratios of the *Escherichia coli* (*E. coli*). They used both INPs capacities as well as UV exposure to decrease the biofouling effect. Finally, reverse osmosis field studies on microbial deactivation revealed less loss of permeability because of the destruction of the microbial cell as well as there was no attachment of bacterial cells after death to the membrane. The schematic representation of the membrane is shown in Figure 4.

Liang Luo et al. [37] used the 40 nm sized TiO_2 in anatase crystal form prepared by the same strategy employed by Kim et al. [38]. The incorporation of INPs modified the hydrophilicity of the poly(ether sulfone) UF membranes because of the interaction between the hydroxyl group of TiO_2 nanoparticle and the sulfone group and ether bond in the poly(ether sulfone) structure by coordination and hydrogen bonding. The separation studies revealed the significant reduction of fouling. Later Hyun-bae et al. [39] used the same strategy for the bioreactor membrane fouling reduction where shear force was generated because of increase in hydrophilicity of the membranes reduced fouling.

Madaeni et al. [40] used polyacrylic acid (PAA) coated INPs in PVDF matrix by two strategies where in one the TiO_2 are self-assembled by acrylic acid and in another strategy, *in-situ* grafting by polymerization of blend solution called as "grafting from" technique and their arrangements are shown in Figure 5. Antifouling properties of the nanocomposite membrane were tested using whey solution. Excellent resistance to fouling was observed in membranes made of functionalized TiO_2 due to high grafting yield and low agglomeration. The presence of the -COOH group of polyacrylic acid on the pores and the surface of the PVDF membrane have prepared appropriate sites for immobilization of the INPs. The "grafting from" technique proved to be more optimal over self-assembly because of the durability of INPs in the surface of the modified membrane. The covalent attachment of the TiO_2 to PAA matrix made it stable even during cleaning of membranes. The flow recovery ratio tremendously increased because of TiO_2 which is mentioned in Figure 5C.

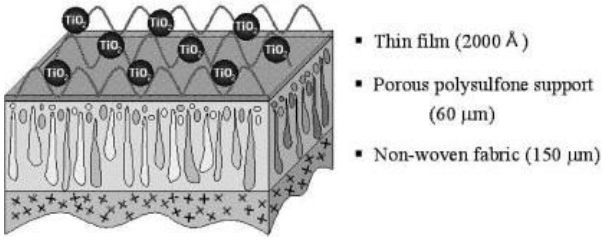

Fig. 4. Schematic representation of hybrid membrane (Reprinted from [36]).

Vatanpour et al. [41] studied the effect of INPs size in the reduction of fouling using P25, PC105, and PC 500 based TiO_2 by blending them into a matrix of polyethersulfone. If the surface hydrophobicity was improved because of INPs incorporation, the high loading of PC105 and PC 500 decreased the performance due to a high level of agglomeration whereas PC 25 shown consistent dispensability. The aggregation of nanoparticles reduced the active surface of nanoparticles and thereby declining in the number of hydroxyl groups on the surface of the membrane. The contact angle was decreased from 65 (for nascent PES membrane) to 49 when the INPs loading was changed from 1 to 4 wt%. The antifouling mechanism was studied using whey solution. The flux recovery percentage of P25/PES membrane was increased from 56 to 91% by blending 4 wt% P25 nanoparticles. The lower concentration of NPs reduces the chances of agglomeration compared to high loading. There is few more literature available which are mainly focused on membrane fouling, and they are detailed in Table 2.

To avoid the agglomeration of the TiO_2 INPs, Teow et al. [42] incorporated the INPs into PVDF matrix via phase separation with colloidal precipitation method with subsequent sonication and precipitation techniques. They found that there is a substantial effect of particle distribution in the matrix by the type of solvent used. The membrane prepared using N-methyl-2-pyrrolidone (NMP) as a solvent has smaller surface particulate matter and narrow particle size distribution compared to N-N-dimethylacetamide (DMAc) and N, N-dimethyl formamide (DMF). This is mainly due to the hydrophobic/ hydrophilic interactions between NPs and polymer solution. Cellular pore structure appeared on the surface of a membrane made from DMF whereas membranes from NMP and DMAc resulted in more connected pores. This was related to solubility parameters of solvent in water. The solubility parameter of water with organic solvent increased from DMF to DMAc and then to NMP.Improved miscibility of DMF with water increased the polymer concentration at the interface due to the higher solvent outflux resulting in tighter pore size. The pore size of membranes prepared from NMP was relatively bigger resulting in a severe rejection of humic acid during filtration. PVDF/TiO_2 mixed matrix membrane using DMAc as a solvent with 0.01 g/L of TiO_2 in the coagulation bath shown good permeability (43.21 L/m^2.h) with excellent retention properties (98.28%) of humic acid. As the TiO_2 concentration in doping solution increased, the hydrophilicity of the membranes were increased, but this might also induce the aggregation of INPs thus blocking the pores of the membrane.

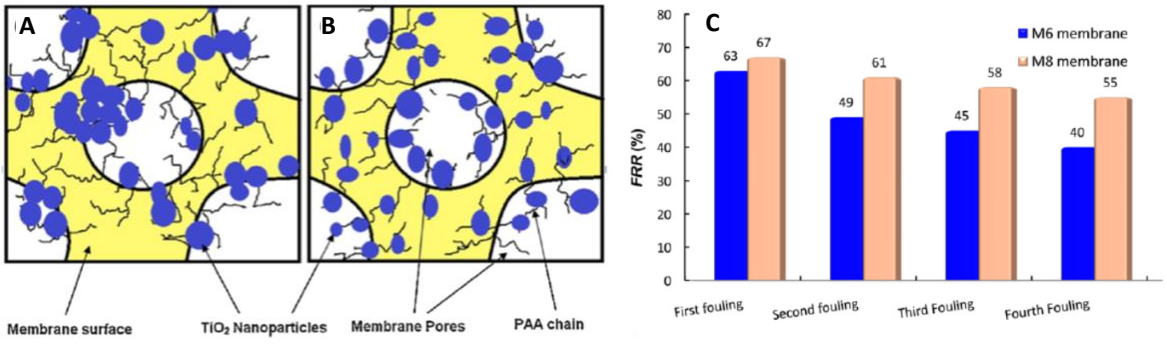

Fig. 5. Schematic of immobilization of TiO_2 nanoparticles in (A) self-assembling method and (B) "grafting from" technique (C) Flow recovery ratio estimation (Reprinted from [40]).

Table 2
Summary of the prepared TiO_2/polymeric membranes in the literature for the antifouling purpose. (Reprinted from [41]).

TiO_2 Type	Size (nm)	Matrix	Preparation of membrane	Type of membrane
Anatase (lab prepared)	10	TFC (PA/PSf)	Self-assembly	RO
Anatase (lab prepared)	5-42	PES	Self-assembly	UF
Anatase (lab prepared)	4-7	Surface sulfonated PES	Self-assembly	MF
Anatase (lab prepared)	4-7	sulfonated PES	Self-assembly	UF
Degussa P25	20	TFC (PA/PSf)	Mixed by PA monomer and polymerized	NF
Degussa P25	20	TFC-SR (PVA top layer)	Self-assembly	RO
Anatase (lab prepared)	10-50	SMA/PVDF blend membrane	Self-assembly	UF
Degussa P25	20	−OH functionalized PES/PI blended membrane	Self-assembly	NF
Degussa P25	20	Regenerated cellulose	Self-assembly	UF
Anatase (China)	80-120	TFC (PAA/PP)	Self-assembly	MF
Degussa P25	20	TFC (PAA/PVDF)	Self-assembly or mixed with monomer	MF
Degussa P25	20	PSf-PVDF-PAN	Blended/deposited	UF
Degussa P25-silane coupling agent modification	20	PES/DMAc/PVP	Blended	UF
Degussa P25	20	Polyamideimide-PVDF	Blended	UF
TiO_2 (Aldrich)	300–400	P84 co-polyimide	Blended	Hollow fiber
Rutile (lab prepared)	26-30	PVDF	Blended	UF
Anatase (Tayca Japan)	180	Poly(vinyl butyral)	Blended	Hollow fiber-MF
Degussa P25	20	PES/DMAc/PVP	Blended	UF
Degussa P25	20	PVDF	Blended	MF
TiO_2 (American Elements)	5	P84 polyimide	Blended	NF
Degussa P25	20	PVDF	Blended	UF
Degussa P25	20	PES/(DegOH: DMAc)	Blended	MF
Sol-gel added/Degussa P25	20	PVDF	Sol–gel/blended	Hollow fiber-UF
Degussa P25	20	PSF	Blended	Hollow fiber-UF
Anatase (lab prepared)	62	Cellulose acetate	Blended	UF
Degussa P25	20	PVDF/SPES/PVP	Blended	UF
Rutile type (China)-silane couple reagent	30	Poly(phthalazine ether sulfone ketone)	Blended	UF
TiO_2 (Haina) modified by sodium dodecyl sulfate	20-30	PSF	Blended	UF
Anatase (lab prepared)	25	PES	Blended	NF
TiO_2 (Sigma-Aldrich) /LiCl.H2O	30	PES/DMAc/PVP	Blended	UF

PA: Polyamide, PAA: Polyacrylic acid, PP: Polypropylene, TFC: Thin film composite, SMA: poly(styrene-alt-maleic anhydride), SPES: sulfonated PES.

Another work showing the surface property change to avoid the aggregation is by Kiadehi et al. [10]. They used the amino functionalized NPs to increase the interaction between the gas molecule and the composite membrane. TiO_2 nanoparticles were pretreated with ethylenediamine (EDA) to synthesize amine functionalized TiO_2 which is then doped in polysulfone (PSf) matrix. The hybrid membrane containing 10 wt% amino-functionalized TiO_2, the permeability of N_2, CH_4, CO_2 and O_2 increased up to 0.69, 0.8, 3.5 and 1.1 GPU respectively. Due to the higher interaction of amine groups on F-nano TiO_2 with polar gasses, amine-functionalized TiO_2 had better permeability and selectivity in comparison to pure TiO_2.

5. Fe_2O_3 and Fe_3O_4 as filler

Iron is most available transition metal posing high magnetic and catalytic activities. In this review, we have discussed some of the critical literature where Iron oxide nanoparticles have been used to synthesize the mixed matrix membrane mainly for waste water treatment and other application. The incorporation of INPs lead to increase in membrane performance with long shelf life as no leaching of INPs have been observed [43].

5.1. Iron nanoparticles in water treatment

The main application of Iron nanoparticles in nanocomposite membrane is to treat the contaminated water where Iron NPs adsorbs contaminant followed by its degradation or just by adsorption and then the contaminant metals are leached out. In 2004, Meyer et al. [26,44] used Ni/Fe NPs in cellulose acetate membrane for trichloroethylene (TCE) degradation which explained in the later section of bi-nanoparticles use in nanocomposite membrane preparation.

Kim et al. [45] produced a cationic exchange membrane (CEM) by incorporating zero valent Iron particles (ZVI) with size varying from 30-40 nm. The microporous CEM was converted into the dense structure by incorporation of Pd-doped ZVI nanoparticles. The membrane showed high reactivity because of increased surface area due to the INPs doping. The removal of trichloroethylene was carried out by sorption on the membrane and degradation by the immobilized ZVI. The new CEM was shown a pore diameter ranging from 8 to 80 nm whereas hybrid membrane exhibited the smaller pore whose size was less than 8 nm which was due to the solvent used for preparation and the borohydride solution. About 36.2 mg/L of TCE was removed within 2 h of the experiment, and the adsorption capacity increased by 2 to 3 times by low metal loading (ca. 6.5 mg/L) as compared to a higher loading of metal (20 g/L).

Xu et al. [46] encapsulated Iron NPs in poly(vinyl pyrrolidone) (PVP) nanofibrous membranes by an electrospinning technology to achieve a catalytic activity for groundwater purification. The composite fibers are fragile with a diameter of about 500 nm containing evenly distributed Iron NPs which reduced the oxidization of Iron because of encapsulation. The catalytic activity was studied using bromate solutions exhibiting about 90% of retained activity compared to bare NPs. The surface area of the electrospun polymeric fibers was controlled by the viscosity of the dope solution, the delivery rate of solution, applied voltage and the distance between the syringe tip and collector. The encapsulation strategy proved to be successful for the protection of iron nanoparticles from oxidation and retaining its catalytical activity.

Tong et al. [47] used the Fe_2O_3 to make mixed matrix membranes with nylon matrix and used them for filtration of ground water contaminated with

nitrobenzene showing 38.9% decrease in nitrobenzene concentration in 20 min of filtration. This is due to the reduction reaction carried out by embedded Iron NPs following pseudo-first-order kinetics. About 72.1% of reduction was observed in the 1st cycle of filtration which was fallen drastically after 5 cycles. After 6 cycles of decline, the immobilized iron nanoparticles lost its reactivity entirely due to the complete leaching out of iron from the membrane. The iron oxide used for composite membrane preparation was not zero valent mainly because of the production environment (not strict anaerobic condition) which is also one of the reasons why the iron NPs lost it reactivity over the filtration cycles.

Daraei et al. [48,49] prepared polyethersulfone (PES) and self-produced polyaniline/iron(II,III)oxide (PANI/Fe_3O_4) nanoparticles based nanocomposite membranes by phase inversion technique. The membranes with 0.01, 0.1 and 1 wt% Iron NPs were produced where the membrane with 0.1 wt% shown higher removal of copper ions from water which was mainly due to the smoother surface of the membrane because of even distribution of the particles which reduced the pore size. The 0.01 wt% concentration was very less, and when the concentrations of INPs increased, the surface roughness enhanced by accumulation and agglomeration of INPs. The higher level mainly produced the hunks since the distance between the NPs is very less. The higher content of INPs developed the hunks due to the decrease of the distance between the INPs. When the concentration of INPs increased, the viscosity of casting solution increased causing the slowdown in phase inversion process. This delay causes the local agglomeration of INPs along with delayed demixing. So the even distribution is critical to have a well accessible active site for copper ion adsorption. Table 3 shows the roughness, water content and the porosity of the composite membrane.

Gholami et al. [50] used (polyvinyl chloride-blend-cellulose acetate/iron oxide nanoparticles) nanocomposite membranes for lead removal from waste water. To change the hydrophobicity of the membranes, they used a different concentration of cellulose acetate like 2.5, 5, 7.5, 10, 15, 25, 50, and 75 wt% where 10% of CA was selected as best concentration. The membranes containing 0.01, 0.1 and 1 wt% of Fe_3O_4 were used to improve membrane rejection. A membrane with 0.1% of Fe_3O_4 showed better flux and rejection compared to others. As the amount of Iron NPs was increased the number of channels across the cross section was increased. As nanoparticles loading was increased, NPs started accumulation creating hunks in the structure of the membrane which has then reduced the salt rejection. 0.01 and 0.1% of NPs in membrane shown 100% rejection of the lead by the membrane. The membrane moisture content was increased as NPs concentration raised to 0.1% and when it reached 1 wt%, the moisture content shown decline trend because of filling of cavities in the membrane by NPs decreasing the free available void which will also affect the mechanical strength of the membrane. The increase of nanoparticle concentration creating more channels in membrane cross section and thereby decreasing the mechanical strength of the membrane.

Ghaemi et al. [51] reported a surface modification of Fe_3O_4 nanoparticles by immobilizing silica, metformine, and amine. Mixed matrix PES nanofiltration membrane was prepared by embedding various concentrations of the modified Fe_3O_4 based nanoparticles as shown in Figure 6. The nanocomposite membrane showed increase water flux because of changes in the mean pore radius, porosity, and hydrophilicity of the membranes. The copper adsorption capacity was dramatically increased because of improved hydrophilicity and also the presence of nucleophilic functional groups on nanoparticles. The nanoparticles in the casting solution also facilitated the solvent (DMAc) diffusion rate from the membrane into the water. This phenomenon decreased the interaction between polymer and water and making easier diffusion of the solvent molecule from the polymer matrix into a coagulation bath. The overall process went the average pore size and porosity of the composite membrane to the higher degree compared to the nascent PES membrane. The hydrophilicity of the membrane was increased with INPs coated with amine and metformin due to the aromatic hydrocarbon. The membrane fabricated with 0.1 wt% metformine-modified silica coated Fe_3O_4 nanoparticles showed the highest copper removal (about 92%) due to high affinity in copper adsorption. The existence of nucleophile group on iron oxide surface increased the adsoprtion capacity of the nanocomposite membrane. The EDTA was used as cleaning agents making the membrane reusable for many cycles.

Table 3
Membrane composition with water content and porosity.

Membrane	Moisture content (Wt%)	Porosity (V/V%)
PES	285	62
FA0.01	293	68
FA0.1	307	71
FA1	328	77

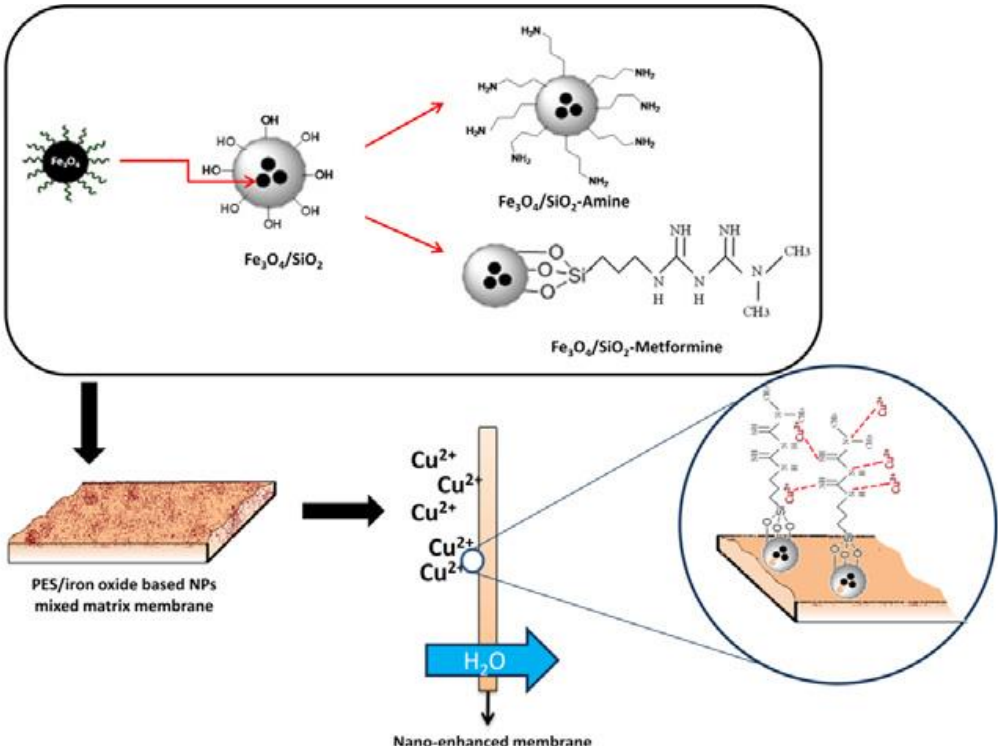

Fig. 6. Synthesis of nanocomposites with surface modified INPs (Reprinted from [51]).

One more strategy to enhance the properties of nanocomposite membrane is to incorporate bimetallic particles instead of single one. There are fewer literature detailed below where the bimetallic approach was used. Meyer et al. [26] used Ni/Fe NPs in cellulose acetate membrane for trichloroethylene (TCE) degradation. Phase inversion method was utilized for the synthesis of membrane containing NPs with size 24 nm. 75% reduction of TCE was achieved by use of 31 mg (24.8 mg Fe, 6.2 mg Ni) of NPs with ratio 4:1 for 4.25 h. The films had a permeability of approximately 3×10^{-7}cm s^{-1} bar^{-1}. The degradation reaction followed pseudo-first order kinetics. There was minimal leaching of NPs into surrounding solution during cleaning.

Wang et al. [52] hydrophilized the PVDF MF membranes with the mixture of polyvinyl alcohol (PVA), glutaraldehyde, and polyethylene glycol (PEG) containing Pd/Fe nanoparticles. The membrane-supported Pd/Fe NPs shown high reactivity in the dechlorination of trichloroacetic acid (TCAA) due to the presence of highly reactive iron site and adsorptive palladium site. The removal efficiency increased to 95.8% with the metal loading of 5.08 mg/13 mL with 30 min reaction time. The mixed matrix membrane showed a complete dechlorination following pseudo first order kinetics. The dechlorination reactivity of NPs remained stable for four cycles and then shown a decline in their catalytic activity. The decrease of activity was related to oxidation of the zero-valent iron and deactivation of Pd due to the coverage of passivation layer.

Later Wu et al. [27] used the combination of Pd/Fe for degradation of trichloroethylene (TCE) from water using MMMs from cellulose acetate. Solution and microemulsion techniques were used to synthesize the iron nanoparticles. Pd/Fe bimetallic particles were prepared by post-coating Pd on the prepared metal nanoparticles and then blended with CA. The Pd/Fe shown size of 10 nm. A comparative study for the Pd/Fe (Pd 1.9 wt%) nanoparticles from solution and microemulsion methods showed that the nanoparticles synthesized from microemulsion technique shown good behavior for the dechlorination of TCE. The studies of TCE degradation revealed that the ratio of the initial TCE concentration to the Pd/Fe particle loading had a significant influence on the observed reduction rate constant when a pseudo-first-order reaction model was used.

Parshetti et al. [53] used the Fe/Ni nanoparticles immobilized in nylon 66 and PVDF membranes used for dechlorination of trichloroethylene (TCE). The particle sizes of Fe/Ni in PVDF and nylon 66 membranes were 81 and 55 nm with the Ni layers of 12 and 15 nm, respectively. Lower levels of agglomeration of immobilized Fe/Ni nanoparticles in nylon 66 membrane was observed which was due to the presence of more multifunctional chelating groups in monomer units of nylon (adipic acid and methylene diamine). The ion exchange, chelation and electrostatic interaction between monomer and metal ions also will play an important role in uniform distribution of the nanoparticles in the final membrane. Quick hydrochlorination of TCE with ethane as the primary end product was followed by the immobilized Fe/Ni nanoparticles with pseudo-first-order Kinetics. When Ni loading was increased from 2.5 to 20 wt%, the dechlorination rate was increased from 77 to 94% with 16 cycles of a lifetime for the catalytic activity of NPs.

Gohari et al. [54] used Fe/Mn NPs in PES matrix to form nanocomposite membranes for the adsorptive elimination of arsenic. The casting solution consisting of Bimetal concentration varying from 0 to 1.5 was used. In this work, ultrafiltration (UF) mixed matrix membranes (MMMs) composed of polyethersulfone (PES) and Fe/Mn binary oxide (FMBO) particles. The increase in hydrophilic FMBO ratio resulted in an increase in thickness of skin layer due to the broadening of miscibility gap in the polymer-solvent-non-solvent diagram. The increased FMBO ratio also caused an increase in viscosity of the polymer solution which slowed down the diffusion of water from the coagulation bath to the cast polymer solution. The hydrophilic nanoparticles acted as a disperser of water into small droplets in the top surface resulting in smaller pores as shown in Figure 7. The incline in membrane water flux mainly due to the increase in contact angle, surface roughness and grown in some pores as shown in SEM picture below (see Figure 7) with its composition mentioned in Table 4. The best performing membrane structure was fixed to 1:5:1 for Fe-Mn-PES showing a water flux of 94.6 $L.m^{-2}.h^{-1}$ at 1 bar of pressure with arsenic removal capacity of 73.5 mg/g. 87.5% membrane adsorption capacity was regenerated with NaOH and NaOCl wash.

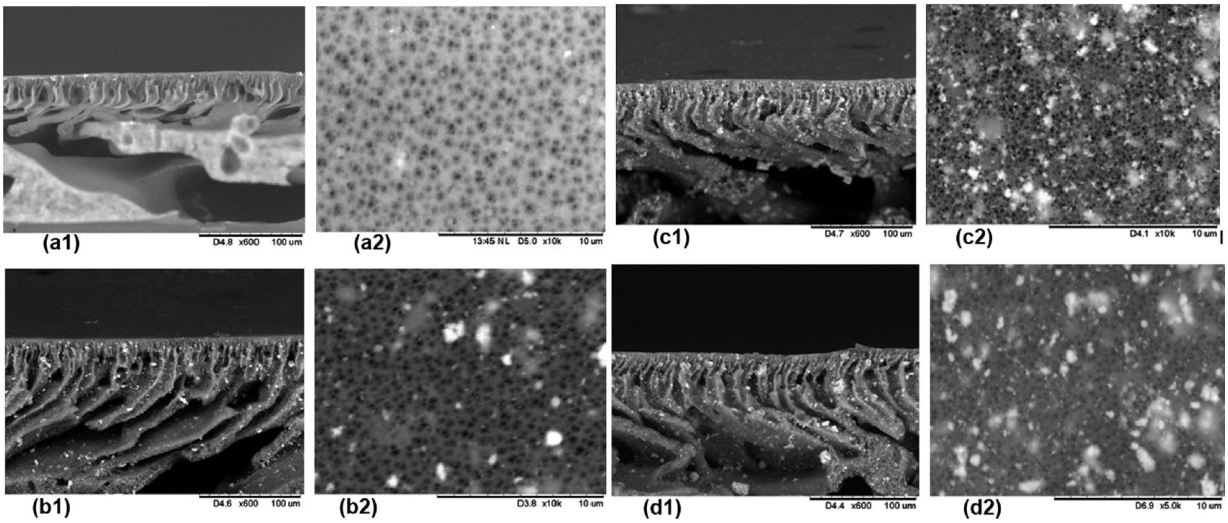

Fig. 7. SEM photographs of the cross section (numbered as 1) and the top surface (numbered as 2) of membranes prepared from different FMBO/PES ratios (a) M0, (b) M0.5, (c) M1.0 and (d) M1.5 membrane. (Reprinted from [54]).

Table 4
Composition and viscosity of casting dope.

Membrane	FMBO/PES ratio	PES (Wt%)	PVP (Wt%)	NMP (Wt%)	FMB0 (Wt%)	Viscosity (cp)
M0 (control)	0.0	15.00	1.5	83.5	-	203
M0.5	0.5	13.95	1.4	77.67	6.98	381
M1.0	1.0	13.04	1.3	72.6	13.04	428
M1.5	1.5	12.24	1.22	68.18	18.36	549

5.2. Iron containing membranes from lithography technique for MEMS application

Pirmoradi et al. [55] Incorporated Iron NPs in PDMS matrix for micro electro mechanical system (MEMS) application. As in the previously reported works, the primary concern was to yield a homogeneous distribution of INPs in the matrix. To reach this objective, the NPs were covered with a hydrophobic coating as well as fatty acids enabling to inhibit the agglomeration. Free-standing magnetic PDMS membranes were fabricated using a combination of micro-molding, sacrificial etching, and bonding techniques. Figure 8 shows the fabrication steps of the free-standing membranes. Initially, the photoresist was deposited on a silicon substrate as a sacrificial layer on which PDMS was spin coated with 3 spinning steps (500 rpm for 15 s, 1000 rpm for 15 s and 2500 rpm for 30 s) and cured at 80 ℃. Arrays of SU-8 pillars with different sizes (4–7 mm diameter) were fabricated on a silicon wafer by photolithography and used as a mold. Later pure PDMS was poured into the mold, cured at 80 ℃ and peeled off from the mold resulting in the formation of cavities in PDMS. Next, this PDMS substrate was permanently bonded to the PDMS magnetic membrane by O_2 plasma treatment of both surfaces using PECVD.

5.3. Casting membrane containing magnetic INPs under magnetic field

Daraei et al. [49] used three different types of INPs as filler to create nanocomposite membranes with PES matrix in N, N-dimethylacetamide (DMAc). The used fillers were neat Fe_3O_4, polyaniline (PANI) coated Fe_3O_4 and Fe_3O_4 coated multi-walled carbon nanotube (MWCNT). The magnetic field casting (0.1 T) improved water flux of the different mixed matrix membranes around 15%, 29% and 96% for Fe_3O_4-MWCNT-PES, PANI-Fe_3O_4-PES, and Fe_3O_4-PES, respectively. Casting under magnetic field caused alignment of the nanofillers in the membrane top-layer and resulted in alteration of the skin-layer morphology and reduced the surface roughness. PANI/Fe_3O_4 mixed membranes showed high hydrophilicity and porous nature of the NPs which improved the antifouling properties. The PANI shell surrounding the INPs facilitated the penetration and the passage of the water through the membrane and increased the water flux in the nanocomposite membrane because of the PANI porous structure and become more hydrophilic when it is mixed with hydrophilic materials like Iron oxide INPs. The membrane surface roughness and hydrophilicity are considered as the crucial factors in fouling reduction. The membrane with smoother and more hydrophilic surface offers lower irreversible fouling and higher flux recovery ratio. The nanocomposite membranes had minimal interaction with whey protein because of higher hydrophilicity resulting in polar- nonpolar interaction between membrane surface and protein and thereby decrease the fouling. The casting under magnetic field also facilitated the even distribution of INPs within membranes making it smoother. The casting of the membrane under magnetic field setup is shown in Figure 9.

5.4. Iron NPs based nanocomposite membranes for pervaporation

Dudek et al. [56] made composite membranes from chitosan with Fe_3O_4 cross-linked by sulphuric acid and glutaraldehyde and used them for pervaporation of water/ethanol mixture. Permeation of water after addition of iron oxide nanoparticles to the polymer matrix for both types of cross-linking agents are gradually increased mainly due to the increase in free volume. The presence of magnetite in the membrane, water become a more preferable medium to pass through it over ethanol. The diffusion coefficient for ethanol and water was larger in membranes containing glutaraldehyde as a crosslinker as compared to membranes cross-linked by sulphuric acid because of a decrease in water adsorption capacity. Table 5 shows the difference between the membrane performances for an increase in Iron NP concentration. The separation factor and selectivity coefficient for sulphuric acid (CHSA) and glutaraldehyde cross-linked (CHGA) membranes are also shown in Table 5.

5.5. Iron nanoparticles with microbial properties

Mukharjee et al. [28] described Iron NP based nanocomposite membranes with polyacrylonitrile UF flat sheet membranes for antimicrobial properties for the first time. About 48 to 65 kDa MWCO membranes were prepared by doping different concentrations (0 to 1 wt%) of INPs shown in Figure 10. The membrane showed a thin and dense top skin layer followed by a porous substructure in the middle and a porous thick layer at the bottom when there are no nanoparticles. The porous substructure has a greater number of pores with circular cross section due to quick demixing and solvent-non-solvent interaction. When the concentration of INPs increased to 0.4 wt%, finger-like pores have been changed to teardrop-like pores (see Figure 10-3g). The number of pores, as well as the sizes, have reduced significantly as INPs loading increased (see Figure 10-3h & 3i). The *Escherichia coli* was used as a model organism to investigate antimicrobial properties of the membrane. The adsorption study revealed that the maximum adsorption capacity of the microorganism by the hybrid membrane was 2.5×10^7 CFU.g^{-1}. The anionic cells of bacteria are electrostatically attracted to cationic INPs impregnated in hybrid membrane causing the degradation of cells (by cell wall rupture). The experimental investigation showed that 0.4 wt% of Fe_3O_4 in a 15 wt% PAN homopolymer was optimal enough to remove the microorganisms and coliforms completely. The INPs reduced the surface roughness of the composite membrane and thereby the biofouling. Leaching of iron oxide nanoparticles from the membrane matrix was not detected.

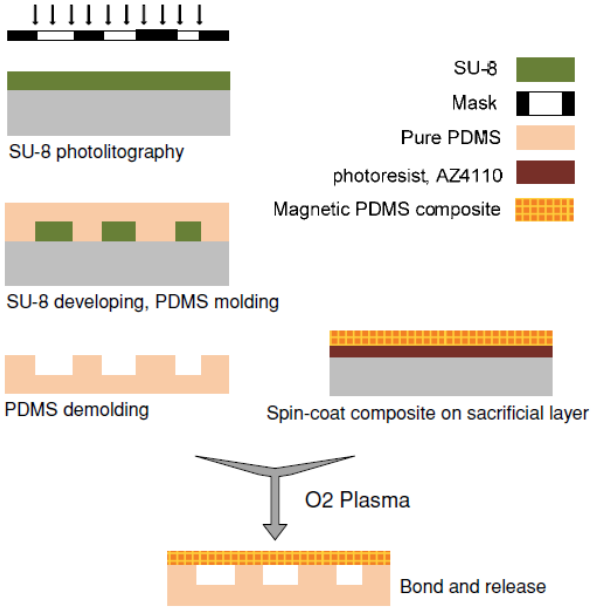

Fig. 8. Synthesis of magnetic membrane (Reprinted from [55]).

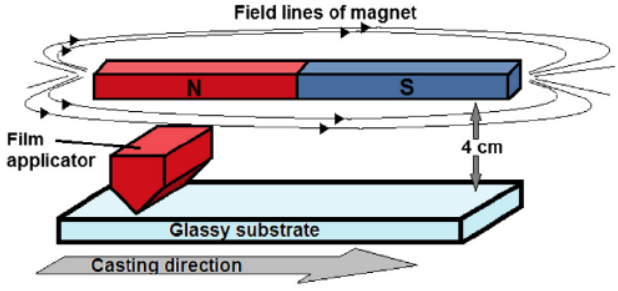

Fig. 9. Casting of membrane under magnetic field (Reprinted from [49]).

Table 5
Separation factor and selectivity coefficients for cross-linked membranes.

	Magnetic Nanoparticle content						
	0%	2%	5%	7%	10%	12%	15%
	CHSA						
Separation Factor	1.0	1.25	1.27	1.31	1.38	1.42	1.43
Selectivity Coeff.	1.02	4.33	4.46	4.5	4.69	4.65	4.67
	CHGA						
Separation Factor	2.6	2.82	2.89	3.02	3.11	3.19	3.27
Selectivity Coeff.	6.52	7.06	7.74	9.43	11.61	12.06	15.28

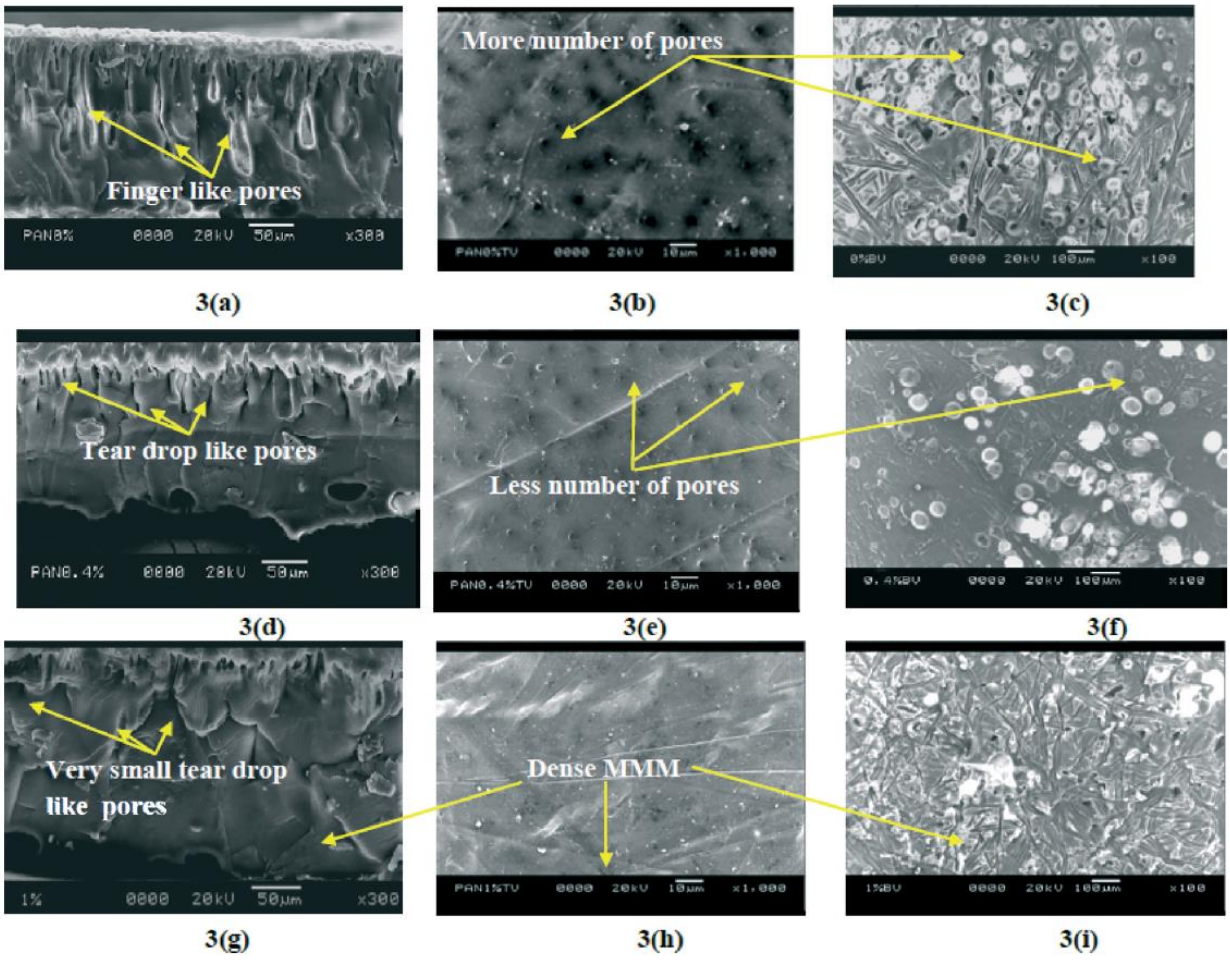

Fig. 10. SEM images of Fe_3O_4–PAN MMMs. (a, d, and g) Cross-sectional views of 0 wt%, 0.4 wt% and 1 wt% MMMs; (b, e, and h) top views of 0 wt%, 0.4 wt% and 1 wt% MMMs; (c, f, and i) bottom views of 0 wt%, 0.4 wt% and 1 wt% MMMs (Reprinted from [28]).

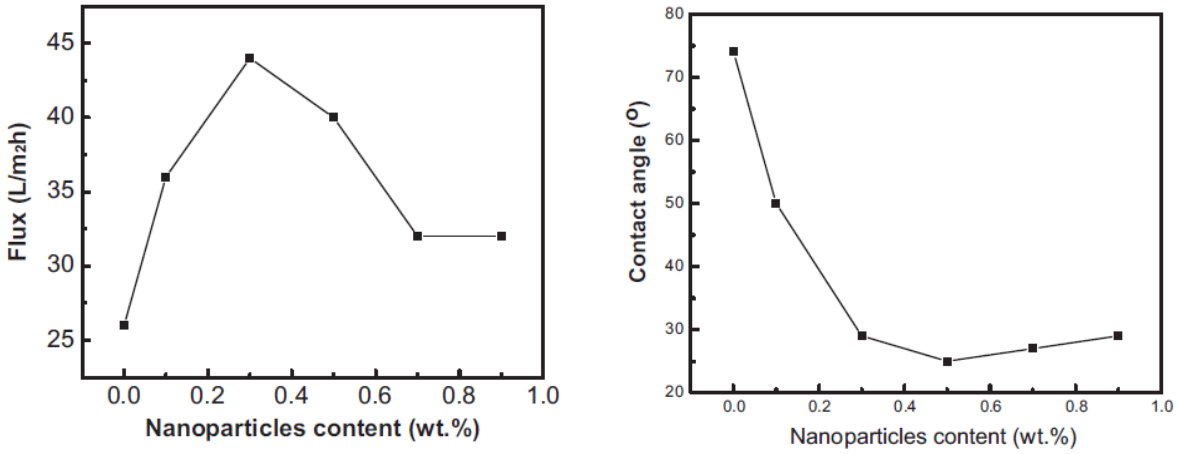

Fig. 11. The flux and contact angle variation with NPs loading (Reprinted from [58]).

5.6. Iron containing membrane as ion exchange barrier

Nemati et al. [57] used Iron NPs functionalized by acrylic acid polymerization and embedded in PAA matrix as cation exchange membranes in THF solvent with cation exchange resin powder as functional group agent. The incorporation of sonication step for the preparation of casting solution lead to a uniform distribution of the INPs and the quick casting lead to superior conducting regions in the membrane for easy flow channels of counter ions. The presence of more conducting regions in the membrane will lead to the uniform electric field across the membrane and thereby decrease the concentration polarization phenomenon. Uniform distribution of the particles also results in improvement in polymer relaxations well as its conformation with particle surface leading to higher membrane selectivity. The membrane water content was decreased from 30 to 17% by an increase of nanoparticle content ratio along with enhancement in membrane hydrophilicity. By increasing the additive concentration, the free spaces in

membrane matrix which is surrounded by INPs resulting in less water accommodation. Additionally, the higher moisture content will provide wider channels for co- and counter ions and decrease the ion selectivity creating a loose structure for the membrane. When NPs load rose to 0.5 wt%, membrane ionic flux and permeability were enhanced which is then decreased as loading increased to 4 wt%. Membrane overall electrical resistance was reduced up to 0.5 wt% of NPs loading and then shown the increasing trend. The prepared membranes showed higher selectivity and low ionic flux at neutral condition compared to other acidic and alkaline conditions.

AL-Hobaib et al. [58] used magnetite iron oxide nanoparticles (γ-Fe_2O_3) with the size of 10 nm in mixed matrix reverse osmosis membrane that was synthesized by interfacial polymerization technique from polysulfone network. The concentration of embedded NPs varied from 0.1 to 0.9 wt% which increases the hydrophilicity of the membrane. At 0.3 wt% of INPs loading the contact angle decreased from 74 to 29 as shown in Figure 11. After 0.5 wt% of addition, the contact angle was almost constant. This is due to the increased ordering of the interfacial water molecules which improves the water molecule's ability to form hydrogen bond and produce stronger interaction between water and the solid surface. The flux and contact angle variation is shown in Figure 11. The permeation test carried out with NaCl solution at a concentration of 2000 ppm, and a pressure of 225 Psi resulted in permeate flux increase from 26 to 44 $L.m^{-2}.h^{-1}$ with 0.3 wt% NPs embedded in the matrix and shown salt rejection of 98%. A decline in flux above 0.3 wt% loading was reported, due to an agglomeration of the NPs resulting in a decrease of the pore size.

6. Silver nanoparticles as filler

The antimicrobial properties of Silver made them very attractive and got demand in industry, food, and medicine [59]. They are embedded in packaging material as sensors to track their lifetime, as a food additive and as juice clarifying agent [30]. In 2005, Bakalgina et al. [60] synthesized the silver membrane for antimicrobial studies and described the effect of the use of Polyvinylpyrrolidone and poviargol on the preparation of silver membranes.

Braud et al. [61] manufactured a bacterial cellulose based silver membrane with a silver particle diameter of 8 nm by soaking *Acetobacter xylinum* culture in the silver solution. Hydrolytic decomposition of Ag–triethanolamine (Ag-TEA) compounds in aqueous solutions at around 50 °C was formed Ag and AgO thin films. TEA acts as a tridentate ligand through two of the three hydroxyl OH groups together with the amine N atom. Ag^+ is reduced to $Ag0_2$ and once these particles were formed, they act as a catalyst for the reduction of the remaining metal ions present in the bulk solution leading to $Ag0_n$ cluster growth.

The electrospun technology is one of the interesting technique to develop silver based nanocomposite membrane showing a higher level of antimicrobial properties. This technology makes the silver NPs stable in final matrix compared to other ionic silver-containing fibers causing the discoloration of tissues [62]. In literature, some examples on the electrospun silver membrane are reported. Jin et al. [63] prepared Ag/poly(vinyl pyrrolidone) (PVP) ultrafine fibers electrospun from the PVP solutions containing AgNPs directly or a reducing agent for the Ag ions. Hong et al. [64] reported that PVA ultrafine fibers containing AgNPs were prepared by electrospinning of PVA/silver nitrate ($AgNO_3$) aqueous solutions, followed by heat treatment. Dong et al.[65] had demonstrated in situ electrospinning method to fabricate semiconductor (Ag_2S) nanostructure on the outer surfaces of PAN nanofibers. Later, Jing et al. [66] synthesized chitosan-poly(ethylene oxide) fibers containing silver NPs by electrospinning in combination with an in-situ chemical reduction of Ag ions. The technique distributed the silver particles evenly in the matrix and the Ag-O bond made the tight interaction between NPs and the matrix. The membrane showed wonderful anti-microbial properties.

Bidault et al. [22,67] used the silver nanoparticles based alkaline fuel cell where silver act as an excellent substrate because of its good electrocatalytic action, a mechanical support and also for its ability to collect the current. The silver based membrane showed the high active surface area of 0.6 m^2g^{-1} which resulted in the excellent electrochemical performance of 200 $mA.cm^{-2}$ at 0.6 V and 400 $mA.cm^{-2}$ at 0.4 V in the presence of 6.9 M potassium hydroxide solution. Figure 12 shows the optical and SEM images of the membrane. Later they modified the membrane by adding catalyst MnO_2 which increased the cathode activity. The modified membrane shown the right results on electrochemical performance which is found to be 55 $mA.cm^{-2}$ at 0.8 V, 295 $mA.cm^{-2}$ at 0.6 V and 630 $mA.cm^{-2}$ at 0.4 V in presence of 6.9 M potassium hydroxide solution. The reason behind the improved electrical performance was due to the increase in hydrophobicity of the membrane because of the addition of catalyst.

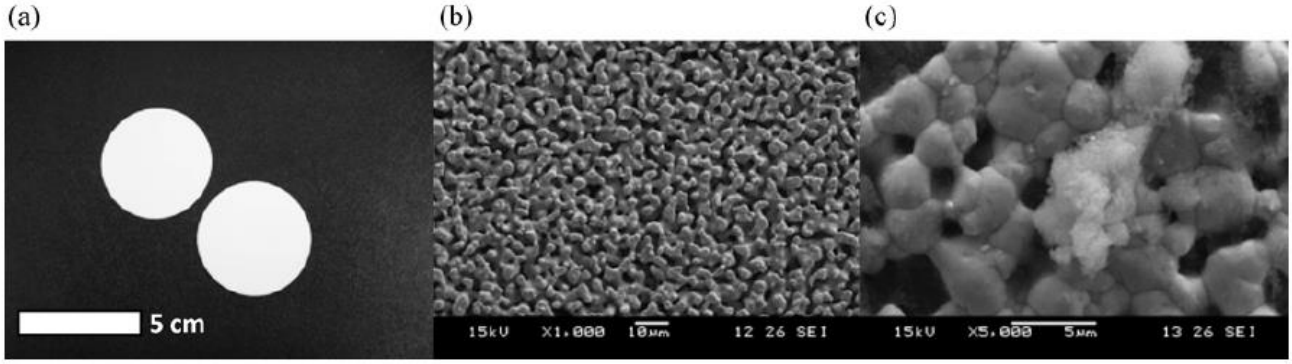

Fig. 12. (a) Optical image of silver membranes; (b-c) SEM images showing the porous structure of silver membranes without (b) and with PTFE (c) (Reprinted from [22]).

As previously discussed, the silver NPs are synthesized by in-situ reduction or they have been added to the polymer solution and then cast to form a hybrid membrane. This method will not show the availability of the embedded silver NPs for any surface based interaction. For the first time, Gunawn et al. [68] developed silver embedded multi-walled carbon nanotube based membrane (shown in Figure 13) which inhibited the growth of bacteria infiltration module and also prevented the formation of biofilm helping in a decrease of fouling. Later Sun et al. [69] used graphene oxide instead of MWCNT which increases the permeation water capacity through the nanocomposite membrane with cellulose acetate matrix. Under filtration condition, the flux drop was 46% for hybrid membrane compared to CA membrane after 24 h of filtration. The composite membrane inactivated 86% of *Escherichia Coli* within 2 h of contact with the membrane. Moreover, higher detachment capacity of the dead cell from membrane surface was found which has decreased the biofouling effect significantly.

7. Conclusions

The addition of inorganic materials to polymeric matrix in the formation nanocomposite membranes offers the promising next generation membranes for both gas and liquid separation. The composite membranes will have the qualities of both materials like good selectivity and permeability, processability and flexibility, chemical and thermal stability and could be synthesized by cost effective strategies. The addition of inorganic fillers like metal oxides and silver NPs increased the performance of the nanocomposite membranes regarding permeability as well as selectivity. Not only the membrane properties but also the particles have provided their characteristics to the composite membrane like magnetic, antimicrobial and catalytic properties helping to solve the problems like membrane fouling, catalytic degradation of pollutant and microorganism inactivation making them most promising future of membrane technology.

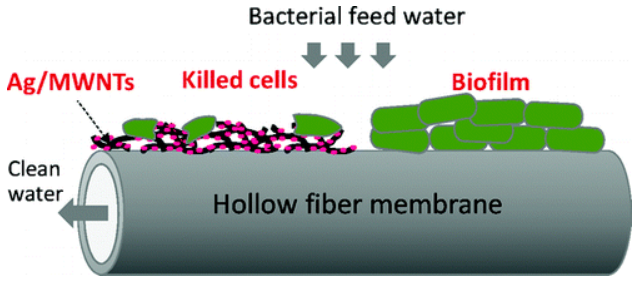

Fig. 13. Schematic representation of silver embedded multiwalled carbon nanotube (Reprinted from [68]).

References

[1] C.M. Zimmerman, A. Singh, W.J. Koros, Tailoring Mixed Matrix Composite Membranes for Gas Separations, J. Membr. Sci. 137 (1997) 145–154.

[2] R.D. Noble, Perspectives on Mixed Matrix Membranes. J. Memb. Sci. 378 (2011) 393–397.

[3] M.A. Aroon, A.F. Ismail, Performance Studies of Mixed Matrix Membranes for Gas Separation: A Review, Sep. Purif. Technol. 75 (2010) 229–242.

[4] J. Kim, B. van der Bruggen, The Use of Nanoparticles in Polymeric and Ceramic Membrane Structures : Review of Manufacturing Procedures and Performance Improvement for Water Treatment, Environ. Pollut. 158 (2010) 2335–2349.

[5] P.S. Goh, A.F. Ismail, S.M. Sanip, B.C. Ng, M. Aziz, Recent Advances of Inorganic Fillers in Mixed Matrix Membrane for Gas Separation, Sep. Purif. Technol. 81 (2011) 243–264.

[6] G. Dong, V. Chen, Challenges and Opportunities for Mixed-Matrix Membranes for Gas Separation, J. Mater. Chem. B 1 (2013) 4610–4630.

[7] S. Kulprathipanja, R.W. Neuzil, N. N. L. US4740219 A, Separation of Fluids by Means of Mixed Matrix Membranes, 1988.

[8] D. Bastani, N. Esmaeili, M. Asadollahi, Journal of Industrial and Engineering Chemistry Polymeric Mixed Matrix Membranes Containing Zeolites as a Filler for Gas Separation Applications: A Review. J. Ind. Eng. Chem. 19 (2013) 375–393.

[9] T. Chung, L. Ying, Y. Li, S. Kulprathipanja, Mixed Matrix Membranes (MMMs) Comprising Organic Polymers with Dispersed Inorganic Fillers for Gas Separation. Prog. Polym. Sci. 32 (2007) 483–507.

[10] A.D. Kiadehi, M. Jahanshahi, A. Rahimpour, A.A. Ghoreyshi, Fabrication and Evaluation of Functionalized Nano-Titanium Membranes for Gas Separation. J. Chem. Eng. 11 (2014) 40–49.

[11] S.M. Momeni, M. Pakizeh, Preparation, Characterization and Gas Permeation Study of PSf / MgO Nanocomposite Membrane. Brazillian J. Chem. Eng. 30 (2013) 589–597.

[12] F. Moghadam, M.R. Omidkhah, M.Z. Pedram, F. Dorosti, The Effect of TiO_2 Nanoparticles on Gas Transport Properties of Matrimid5218-Based Mixed Matrix Membranes. Sep. Purif. Technol. 77 (2011) 128–136.

[13] B. Mccool, G. Xomeritakis, Y.S. Lin, Composition Control and Hydrogen Permeation Characteristics of Sputter Deposited Palladium ± Silver Membranes. J. Membr. 161 (1999) 67–76.

[14] A. Rybak, Z.J. Grzywna, P. Sysel, Mixed Matrix Membranes Composed of Various Polymer Matrices and Magnetic Powder for Air Separation. Sep. Purif. Technol. 118 (2013) 424–431.

[15] P. Safaei, A. Marjani, M. Salimi, Mixed Matrix Membranes Prepared from High Impact Polystyrene with Dispersed TiO_2 Nanoparticles for Gas Separation. J. nanostructure 6 (2016) 74–79.

[16] A. Rybak, G. Dudek, M. Krasowska, A. Strzelewicz, Z.J. Grzywna, Separation Science and Technology Magnetic Mixed Matrix Membranes Consisting of PPO Matrix and Magnetic Filler in Gas Separation Magnetic Mixed Matrix Membranes Consisting of PPO Matrix and Magnetic Filler in Gas Separation. Sep. Sci. Technol. 49 (2014) 1729–1735.

[17] L. Chunqing, S. Kulprathipanja, A.M.W. Hillock, S. Husain, W.J. Koros, Recent Progress in Mixed-Matrix Membranes, in: N.L. Norman, F. Anthony, W. Winston Ho, T. Matsuura (Eds.), Advanced Membrane Technology and Applications, John Wiley & Sons, Inc., 2008, pp. 790–819.

[18] M. Sairam, M.B. Patil, R.S. Veerapur, S.A. Patil, T.M. Aminabhavi, Novel Dense Poly(Vinyl Alcohol)–TiO_2 Mixed Matrix Membranes for Pervaporation Separation of Water – Isopropanol Mixtures at 30°C. J. Membr. Sci. 281 (2006) 95–102.

[19] I. Soroko, A. Livingston, Impact of TiO_2 Nanoparticles on Morphology and Performance of Crosslinked Polyimide Organic Solvent Nanofiltration (OSN) Membranes. J. Membr. Sci. 343 (2009) 189–198.

[20] T. Bae, T. Tak, Preparation of TiO_2 Self-Assembled Polymeric Nanocomposite Membranes and Examination of Their Fouling Mitigation Effects in a Membrane Bioreactor System. J. Membr. Sci. 266 (2005) 1–5.

[21] J. Alam, L.A. Dass, M. Ghasemi, M. Alhoshan, Synthesis and Optimization of PES-Fe_3O_4 Mixed Matrix Nanocomposite Membrane: Application Studies in Water Purification. Polym. Compos. (2013) 1–8.

[22] F. Bidault, A.A. Kucernak, Novel Cathode for Alkaline Fuel Cells Based on a Porous Silver Membrane. J. Power Sources 195 (2010) 2549–2556.

[23] P.S. Goh, A.F. Ismail, B.C. Ng, Carbon Nanotubes for Desalination: Performance Evaluation and Current Hurdles. Desalination 308 (2013) 2–14.

[24] P.S. Goh, A.F. Ismail, Graphene-Based Nanomaterial: The State-of-the-Art Material for Cutting Edge Desalination Technology. Desalination 356 (2015) 115–128.

[25] K.A. Mahmoud, B. Mansoor, A. Mansour, M. Khraisheh, Functional Graphene Nanosheets: The next Generation Membranes for Water Desalination. Desalination 356 (2015) 208–225.

[26] D.E. Meyer, K. Wood, L.G. Bachas, D. Bhattacharyya, Degradation of Chlorinated Organics by Membrane-Immobilized Nanosized Metals. Environ. Prog. 23 (2004) 232–242.

[27] L. Wu, S.M.C. Ritchie, Enhanced Dechlorination of Trichloroethylene by Pd-Coated Iron Nanoparticles. Environ. Prog. 27 (2008) 218–224.

[28] M. Mukherjee, S. De, Environmental Science Drinking Water Using an Iron Oxide Nanoparticle. Environ. Sci. Water Res. Technol. 1 (2015) 204–217.

[29] C. Liu, S. Kulprathipanja, A.M.W. Hillock, S. Husain, W.J. Koros, Recent Progress in Mixed-Matrix Membranes, in: Advanced Membrane Technology and Applications, John Wiley & Sons, Inc., Hoboken, NJ, USA, pp. 787–819.

[30] S. Gaillet, J. Rouanet, Silver Nanoparticles: Their Potential Toxic Effects after Oral Exposure and Underlying Mechanisms – A Review. Food Chem. Toxicol. 77 (2015) 58–63.

[31] S.S. Hosseini, Y. Li, T.-S. Chung, Y. Liu, Enhanced Gas Separation Performance of Nanocomposite Membranes Using MgO Nanoparticles. J. Memb. Sci. 302 (2007) 207–217.

[32] S. Matteucci, R.D. Raharjo, V.A. Kusuma, S. Swinnea, B.D. Freeman, Gas Permeability, Solubility, and Diffusion Coefficients in 1,2-Polybutadiene Containing Magnesium Oxide. Macromolecules 41 (2008) 2144–2156.

[33] S. Matteucci, V.A. Kusuma, S.D. Kelman, B.D. Freeman, Gas Transport Properties of MgO Filled poly(1-Trimethylsilyl-1-Propyne) Nanocomposites. Polymer. 49 (2008) 1659–1675.

[34] F. Mohd Nor, R. Othaman, Effects of MgO Particle Loading on Gas Permeation Properties of Epoxidized Natural Rubber (ENR)/Polyvinyl Chloride (PVC) Membrane. Sains Malaysiana 44 (2015) 875–881.

[35] S. Matteucci, V.A. Kusuma, D. Sanders, S. Swinnea, B.D. Freeman, Gas Transport in TiO_2 Nanoparticle-Filled poly(1-Trimethylsilyl-1-Propyne). J. Memb. Sci. 307 (2008) 196–217.

[36] S.-Y. Kwak, S.H. Kim, S.S. Kim, Hybrid Organic/Inorganic Reverse Osmosis (RO) Membrane for Bactericidal Anti-Fouling. 1. Preparation and Characterization of TiO_2 Nanoparticle Self-Assembled Aromatic Polyamide Thin-Film-Composite (TFC) Membrane. Environ. Sci. Technol. 35 (2001) 2388–2394.

[37] M. Luo, J. Zhao, W. Tang, C. Pu, Hydrophilic Modification of Poly(Ether Sulfone) Ultrafiltration Membrane Surface by Self-Assembly of TiO_2 Nanoparticles. Appl. Surf. Sci. 249 (2005) 76–84.

[38] S.H. Kim, S.-Y. Kwak, B.-H. Sohn, T.H. Park, Design of TiO_2 Nanoparticle Self-Assembled Aromatic Polyamide Thin-Film-Composite (TFC) Membrane as an Approach to Solve Biofouling Problem. J. Memb. Sci. 211 (2003) 157–165.

[39] T.-H. Bae, T.-M. Tak, Preparation of TiO_2 Self-Assembled Polymeric Nanocomposite Membranes and Examination of Their Fouling Mitigation Effects in a Membrane Bioreactor System. J. Memb. Sci. 266 (2005) 1–5.

[40] S.S. Madaeni, S. Zinadini, V. Vatanpour, A New Approach to Improve Antifouling Property of PVDF Membrane Using in Situ Polymerization of PAA Functionalized TiO_2 Nanoparticles. J. Memb. Sci. 380 (2011) 155–162.

[41] V. Vatanpour, S. Siavash, A. Reza, E. Salehi, S. Zinadini, H. Ahmadi, TiO_2 Embedded Mixed Matrix PES Nanocomposite Membranes: Influence of Different Sizes and Types of Nanoparticles on Antifouling and Performance. Desalination 292 (2012) 19–29.

[42] Y.H. Teow, A.L. Ahmad, J.K. Lim, B.S. Ooi, Preparation and Characterization of PVDF / TiO_2 Mixed Matrix Membrane via in Situ Colloidal Precipitation Method. Desalination 295 (2012) 61–69.

[43] P. Jian, H. Yahui, W. Yang, L. Linlin, Preparation of Polysulfone – Fe_3O_4 Composite Ultrafiltration Membrane and Its Behavior in Magnetic Field. J. Memb. Sci. 284 (2006) 9–16.

[44] D.E. Meyer, D. Bhattacharyya, Impact of Membrane Immobilization on Particle Formation and Trichloroethylene Dechlorination for Bimetallic Fe/Ni Nanoparticles in Cellulose Acetate Membranes. J. Phys. Chem. B 111 (2007) 7142–7154.

[45] H. Kim, H. Hong, Y. Lee, H. Shin, J. Yang, Degradation of Trichloroethylene by Zero-Valent Iron Immobilized in Cationic Exchange Membrane. Desalination 223 (2008) 212–220.

[46] X. Xu, Q. Wang, H. Chul, Y. Ha, Encapsulation of Iron Nanoparticles with PVP Nanofibrous Membranes to Maintain Their Catalytic Activity. J. Memb. Sci. 348 (2010) 231–237.

[47] M. Tong, S. Yuan, H. Long, M. Zheng, L. Wang, J. Chen, Reduction of Nitrobenzene in Groundwater by Iron Nanoparticles Immobilized in PEG / Nylon Membrane. J. Contam. Hydrol. 122 (2011) 16–25.

[48] P. Daraei, S. Siavash, N. Ghaemi, E. Salehi, M. Ali, R. Moradian, B. Astinchap, Novel Polyethersulfone Nanocomposite Membrane Prepared by PANI/Fe_3O_4 Nanoparticles with Enhanced Performance for Cu(II) Removal from Water. J. Memb. Sci. 415-416 (2012) 250–259.

[49] P. Daraei, S. Siavash, N. Ghaemi, M. Ali, B. Astinchap, Separation and Purification Technology Fouling Resistant Mixed Matrix Polyethersulfone Membranes Blended with Magnetic Nanoparticles: Study of Magnetic Field Induced Casting. Sep. Purif. Technol. 109 (2013) 111–121.

[50] A. Gholami, A. R. Moghadassi, S.M. Hosseini, S. Shabani, F. Gholami, Preparation and Characterization of Polyvinyl Chloride Based Nanocomposite Nanofiltration-Membrane Modified by Iron Oxide Nanoparticles for Lead Removal from Water. J. Ind. Eng. Chem. 20 (2014) 1517–1522.

[51] N. Ghaemi, S.S. Madaeni, P. Daraei, H. Rajabi, S. Zinadini, A. Alizadeh, R. Heydari, M. Beygzadeh, S. Ghouzivand, Polyethersulfone Membrane Enhanced

with Iron Oxide Nanoparticles for Copper Removal from Water: Application of New Functionalized Fe_3O_4 Nanoparticles. Chem. Eng. J. 263 (2015) 101–112.

[52] X. Wang, C. Chen, H. Liu, J. Ma, Preparation and Characterization of PAA/PVDF Membrane-Immobilized Pd/Fe Nanoparticles for Dechlorination of Trichloroacetic Acid. Water Res. 42 (2008) 4656–4664.

[53] G.K. Parshetti, R. Doong, Dechlorination of Trichloroethylene by Ni/Fe Nanoparticles Immobilized in PEG/PVDF and PEG/Nylon 66 Membranes. Water Res. 43 (2009) 3086–3094.

[54] R.J. Gohari, W.J. Lau, T. Matsuura, A.F. Ismail, Fabrication and Characterization of Novel PES/Fe–Mn Binary Oxide UF Mixed Matrix Membrane for Adsorptive Removal of As(III) from Contaminated Water Solution. Sep. Purif. Technol. 118 (2013) 64–72.

[55] F.N. Pirmoradi, L. Cheng, M. Chiao, A Magnetic Poly(dimethylesiloxane) Composite Membrane Incorporated with Uniformly Dispersed, Coated Iron Oxide Nanoparticles. J. Micromechanics Microengineering 20 (2010) 1–8.

[56] G. Dudek, M. Gnus, R. Turczyn, A. Strzelewicz, M. Krasowska, Pervaporation with Chitosan Membranes Containing Iron Oxide Nanoparticles. Sep. Purif. Technol. 133 (2014) 8–15.

[57] M. Nemati, S.M. Hosseini, Fabrication and Electrochemical Property Modification of Mixed Matrix Heterogeneous Cation Exchange Membranes Filled with Fe_3O_4/PAA Core-Shell Nanoparticles. Ionics 22 (2016) 899-909.

[58] A.S. Al-hobaib, K.M. Al-sheetan, L.El. Mir, Materials Science in Semiconductor Processing Effect of Iron Oxide Nanoparticles on the Performance of Polyamide Membrane for Ground Water Purification. Mater. Sci. Semicond. Process. 42 (2016) 107–110.

[59] N.A. Luechinger, S.G. Walt, W.J. Stark, Printable Nanoporous Silver Membranes. Chem. Mater. 22 (2010) 4980–4986.

[60] Y.G. Baklagina, A.K. Khripunov, A.A. Tkachenko, V.V. Kopeikin, N.A. Matveeva, V.K. Lavrent'ev, V.K. Nilova, T.E. Sukhanova, R.Y. Smyslov, I.S. Zanaveskina, et al. Sorption Properties of Gel Films of Bacterial Cellulose. Russ. J. Appl. Chem. 78 (2005) 1176–1181.

[61] H.S. Barud, C. Barrios, T. Regiani, R.F.C. Marques, M. Verelst, J. Dexpert-ghys, Y. Messaddeq, S.J.L. Ribeiro, Self-Supported Silver Nanoparticles Containing Bacterial Cellulose Membranes. Mater. Sci. Eng. 28 (2008) 515–518.

[62] D. Lee, R.E. Cohen, M.F. Rubner, Antibacterial Properties of Ag Nanoparticle Loaded Multilayers and Formation of Magnetically Directed Antibacterial Microparticles. Langmuir 21 (2005) 9651–9659.

[63] W.-J. Jin, H.K. Lee, E.H. Jeong, W.H. Park, J.H. Youk, Preparation of Polymer Nanofibers Containing Silver Nanoparticles by Using Poly(N-Vinylpyrrolidone). Macromol. Rapid Commun. 26 (2005) 1903–1907.

[64] K.H. Hong, J.L. Park, I.H. Sul, J.H. Youk, T.J. Kang, Preparation of Antimicrobial Poly(vinyl Alcohol) Nanofibers Containing Silver Nanoparticles. J. Polym. Sci. Part B Polym. Phys. 44 (2006) 2468–2474.

[65] F. Dong, Z. Li, H. Huang, F. Yang, W. Zheng, C. Wang, Fabrication of Semiconductor Nanostructures on the Outer Surfaces of Polyacrylonitrile Nanofibers by in-Situ Electrospinning. Materials Letters 61 (2007) 2556–2559.

[66] J. An, H. Zhang, J. Zhang, Y. Zhao, Preparation and Antibacterial Activity of Electrospun Chitosan/Poly(Ethylene Oxide) Membranes Containing Silver Nanoparticles. Colloid Polym. Sci. 287 (2009) 1425–1434.

[67] F. Bidault, A. Kucernak, Cathode Development for Alkaline Fuel Cells Based on a Porous Silver Membrane. J. Power Sources 196 (2011) 4950–4956.

[68] P. Gunawan, C. Guan, X. Song, Q. Zhang, S.S.J. Leong, C. Tang, Y. Chen, M.B. Chan-Park, M.W. Chang, K. Wang, et al. Hollow Fiber Membrane Decorated with Ag/MWNTs: Toward Effective Water Disinfection and Biofouling Control. ACS Nano 5 (2011) 10033–10040.

[69] X. Sun, J. Qin, P. Xia, B. Guo, C. Yang, C. Song, S. Wang, Graphene Oxide – Silver Nanoparticle Membrane for Biofouling Control and Water Purification. Chem. Eng. J. 281 (2015) 53–59.